The hydrothermal melting of low and high albite

JULIAN R. GOLDSMITH AND DAVID M. JENKINS[1]

Department of the Geophysical Sciences
University of Chicago
5734 South Ellis Avenue
Chicago, Illinois 60637

Abstract

The hydrothermal (water saturated) melting curves of both high and low albite have been experimentally investigated to determine the effect of Al/Si ordering on melting relations. The melting behavior of low albite had not previously been examined. At pressures above 4 kbar and temperatures below 760°C, the melting curves of low and high albite diverge steadily with increasing pressure; at 14 kbar the temperature difference is about 30°C, with the curve for low albite at higher temperatures than that of high albite. At pressures greater than 14 kbar both curves display a marked decrease in their dP/dT slopes, and at the higher pressures there is a profound change in the texture of the quenched melt product, from a coherent glass to a finely divided or granular amorphous material. It is suggested that this behavior indicates a fundamental change in the nature of the albite melt, and that at pressures above 14 kbar the melt is highly hydrated and depolymerized. At pressures below 4 kbar and temperatures above 760°C, the melting curves of high and low albite converge and remain essentially indistinguishable up to the highest temperatures investigated (1000°C, 0.25 kbar). The influence of the ordering state of albite on its melting behavior is particularly evident for low albite in the temperature range 740–760°C where there is a time (2–7 day) dependence on the extent of melting. The results of this study cast a new light on the properties of hydrous albitic melts under lower crustal and upper mantle conditions and on the interplay between structural state and temperature of hydrothermal melting.

Introduction

The hydrothermal melting of albite is a subject of considerable interest to geologists, for it serves as a good starting point for understanding the effect of water on the formation of granitic melts. Experimental studies by Goranson (1938), Yoder (1955), Tuttle and Bowen (1958), Luth et al. (1964), Boettcher and Wyllie (1969), Morse (1970), Burnham and Davis (1974), and Bohlen et al. (1982) have all demonstrated a very strong decrease in the temperature of vapor-saturated melting with increase in pressure and have all produced curves that are in approximate agreement. Each of these studies, however, has dealt only with a substantially Al/Si disordered form of albite (high albite) and not with the geologically more relevant Al/Si ordered form (low albite). Given the large differences in the melting temperatures of stable and metastable forms of certain substances, such as quartz (<1500°C) relative to cristobalite (1713°C) (Sosman, 1927), it was felt desirable to compare the hydrothermal melting of low and high albite. Furthermore, it was thought that additional information on the high–low albite relations might be obtained, sup-

plementing that reported by Goldsmith and Jenkins (1985) in the preceding article.

Figure 1 is a diagrammatic representation of the polybaric hydrothermal melting behavior of two modifications of a substance such as albite in which the liquid takes H_2O in solution but the solid does not. For both modifications the melting temperatures are lowered with increasing $P(H_2O)$. However, the dP/dT slopes of the two melting curves differ at a given pressure depending on the differences in the Gibbs free energies of the two solids (assuming the liquids to be equivalent). The curves cross at the pressure and temperature (T_r) where the two modifications are in equilibrium. At temperatures lower than the transition temperature T_r high albite is metastable with respect to low albite, and the melting curve of high albite (dashed curve) lies at lower temperatures than that of low albite (solid curve). At temperatures above T_r the opposite situation exists. To simplify the above discussion a first-order transformation was assumed instead of the "non-first" order transformation determined for albite by Goldsmith and Jenkins (1985). A non-first order transformation would produce a *range* of pressures and temperatures over which the two curves would coincide before diverging.

In this study the melting relations of natural low albite have been investigated as a function of $P(H_2O)(= P_{total})$

---

[1] Current address: Department of Geological Sciences, State University of New York-Binghamton, Binghamton, New York 13901.
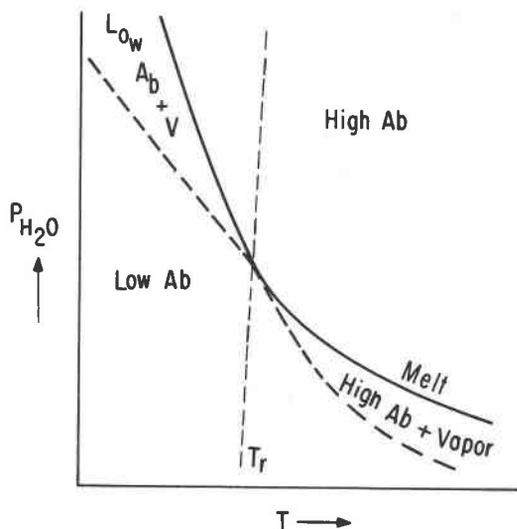
Fig. 1. Diagrammatic representation of polybaric hydrothermal melting relations of two modifications of a substance in which the liquid takes H_2O in solution, whereas the solid does not. A first-order transformation is represented, and the intersection of the curves marks the equilibrium temperature of the transition (T_r) at that pressure. Metastable extensions are shown as dashed curves. If this were the situation for albite, the low albite melting curve would be the solid line below T_r, and the dashed line at higher temperatures; the high albite melting curve solid at temperatures greater than T_r, and dashed at lower temperatures.

and of time. In addition, the curve for high albite was concurrently re-investigated.

Experimental methods

Apparatus and techniques

The experimental apparatus and techniques (piston-cylinder apparatus and internally heated argon pressure vessels) are essentially the same as those described in the preceding article (Goldsmith and Jenkins, 1985) with a few exceptions. In the hydrothermal runs made at relatively high temperatures and low pressures (less than ~1 kbar), it was necessary to limit the amount of water in the sealed capsule to avoid puffing or bursting. The amount of water needed was determined from steam tables after calculation of the capsule volume, including its contents, and the water was carefully added with a microliter syringe. Leakage was checked by weighing the capsule before and after the run.

In experiments in the $P(H_2O)$–T regions where the melting behavior of high albite and low albite could be directly compared, samples of both polymorphs were run adjacent to each other. As many as four capsules could be accommodated in the gas vessels, and one or two, rarely three, in the solid media devices.

Analytical techniques

All of the hydrothermal runs were examined under the petrographic microscope. A JEOL JSM-35 scanning electron microscope was used to examine selected run products. Relative proportions of crystals and glass in runs that were partially melted are based on best estimates, by eye, under the microscope. Whenever

possible, the estimate was also based on the intensities of the X-ray diffraction pattern relative to scans of crystalline albite. Measurements of the Al/Si ordering were made on some run products by measuring the $\Delta 2\theta 131$–$1\bar{3}1$ (or simply $\Delta 131$) from the X-ray diffraction pattern as described by Goldsmith and Jenkins (1985).

Starting materials

Three natural low albites [LoAb(a), LoAb(b), LoAb(c)] and three synthetic high albites [HiAb(a), HiAb(b), HiAb(c)] were used in this study and are described in detail by Goldsmith and Jenkins (1985). To evaluate the effect of any slight but possibly significant compositional difference between the low albite and synthetic high albite used, two samples of LoAb(a) were converted to high albite by heating at 1200°C and 20 kbar for six days ($\Delta 131$ = 1.96, 1.98), to be used for comparison experiments, and are designated in Table 1 as MAb-15 and MAb-20.

Experimental results

Criteria for hydrothermal melting

Glass and crystals of albite are observed to coexist in quenched hydrothermal experiments. Tuttle and Bowen (1958) reported that albite melts over a temperature range of 10°C or more, and ascribed the melting interval to several possibilities: (1) the liquid and/or the vapor had compositions off the binary join albite–water, (2) equilibrium was not reached in their runs, or (3) there was solid solution of water in albite. Tuttle and Bowen (1958) noted that the beginning of melting was sharp, and that approximately 90% glass was formed in a temperature interval of 10°C.

The question of equilibrium is of interest. Many of the samples run for a matter of hours, or in some cases, even days, are glassy 'slugs", with clear to bubbly outer layers, and a core of crystals and lesser glass. It would appear that melting which may begin throughout the compressed powdered charge is suppressed in the water-depleted interior of the sample by a layer of glass through which water must diffuse. This effect was observed by Burnham and Jahns (1962), who, in measuring the solubility of water in silicate melts, state, "It is extremely important that each melt be compositionally uniform, and in particular that the introduced water be uniformly distributed through it; otherwise crystals invariably form in local domains that are undersaturated with respect to water, even though the melt as a whole might be oversaturated." A number of the runs in this study that show crystalline material encased in glass are not equilibrated from this point of view. However, since the "solidus", or beginning of melting is used in this work, no effort was made to determine the equilibrium liquidus.

The suggestion by Tuttle and Bowen (1958) that the composition of the liquid or vapor might not lie on the binary join $NaAlSi_3O_8$–H_2O is reasonable. We see no compelling argument for congruent solubility of multicomponent phases. Morey (1957) presents data on albite at 500°C and 400, 1000, and 2000 bars $P(H_2O)$ indicating that the material transported by steam at 400 bars contains alkali oxide and silica in excess of the feldspar ratio, and

the remaining material contains an excess of alumina. At 2000 bars, however, the ratio is closer to congruency. A rather small deviation from congruent solubility might well account for the 5–15°C melting interval observed in albite.

High albite

Hydrothermal melting of (high) albite has been studied by Goranson (1938), Yoder (1958), Tuttle and Bowen (1958), Luth et al. (1964), Boettcher and Wyllie (1969), Morse (1970), Burnham and Davis (1974), and Bohlen et al. (1982). To ensure direct comparison with low albite, the melting curve of high albite from 16 kbar to less than 1 kbar was re-investigated. The data are in Table 1 and plotted in Figure 2.

A number of experiments were made to evaluate the effect of time on the location of the solidus, but run duration from 1 to 350 hours produced the same results. We also found no significant difference in the melting of the synthetic high albite and the high albite prepared by disordering LoAb(a). Our curve is in rather good agreement (within ~10°C) with Tuttle and Bowen (1958), particularly at the lower pressures, in excellent agreement with Burnham and Jahns (1962) and with Boettcher and Wyllie (1969) at 10 kbar, but is significantly lower (~20°C) than Luth et al. (1964) at 8 and 10 kbar, and is significantly higher than Bohlen et al. (1982) in the range 5–10 kbar. The latter reference discusses (p. 454) the comparative data of previous investigators. Bohlen et al. (1982) point out that

Table 1. Hydrothermal melting data

Run # MAb-	Starting material	T°C	P, kbar	Time, hrs.	Results[*]
154	LoAb(a)	630	19	1.5	Ab, quench fluid, some jadeite
153	LoAb(a)	630	18	1.5	Ab, quench fluid
165	LoAb(a)	600	18½	1.5	Ab, pure jadeite
166	LoAb(a)	610	18½	1.5	Ab, quench fluid, rare jadeite
164	HiAb(b)	600	17	1.5	quench fluid, Ab
155	LoAb(a)	630	17	1.5	all Ab
137	LoAb(a)	650	17	1.5	Ab, some quench fluid
133	LoAb(a)	660	17	1.5	Ab, quench fluid
108	LoAb(a)	670	17	1	quench fluid, some Ab
105	LoAb(a)	680	17	3.25	quench fluid, trace Ab
162	HiAb(a)	600	16	1.5	Ab, quench fluid
111	HiAb(a)	640	16	1.5	quench fluid, some Ab
146	LoAb(a)	660	16	1.5	all Ab
147	LoAb(a)	670	16	1.5	quench fluid, Ab
163	HiAb(a)	600	15	1.5	all Ab
160	HiAb(a)	630	15	1.5	Ab, sparse quench fluid
156	HiAb(a)	640	15	1.5	Ab, quench fluid
149	LoAb(a)	670	15	1.5	all Ab
148	LoAb(a)	680	15	1.5	Ab, quench fluid
25	HiAb(a)	660	14	2	xls, v. small amount glass 1.85
6b	HiAb(a)	670	14	1	glass + minor xls
6a	LoAb(a)	670	14	1	all xls
30	LoAb(a)	680	14	1.5	all xls
104a	LoAb(a)	685	14	2	all xls
104b	LoAb(c)	685	14	2	all xls
9	LoAb(a)	690	14	1	xls, small amount glass 1.08
16	LoAb(a)	700	14	1	glass, some remaining xls
32a	HiAb(a)	680	11	1.5	all xls
32b	MAb-20	680	11	1.5	all xls
26a	HiAb(a)	690	11	1.5	xls + glass (~ 50–50)
26b	MAb-20	690	11	1.5	xls + small amount glass
36a	MAb-20	700	11	1.5	all glass
36b	HiAb(a)	700	11	1.5	all glass
57	LoAb(a)	700	11	77	xls, rare glass 1.12
28b	MAb-20	705	11	1.5	all glass
28a	LoAb(a)	705	11	1.5	xls, v. small amount glass
34	LoAb(a)	720	11	1	all glass
86a	LoAb(a)	722	8.05	240	xls, v. small amount glass
2a	LoAb(a)	685	8	1	all xls
2b	HiAb(a)	685	8	1	all xls
3	LoAb(a)	700	8	1	all xls 1.08
55	HiAb(a)	700	8	72	all xls 1.87
23	HiAb(a)	710	8	1.5	xls, v. small amount glass 1.90
4a	LoAb(a)	715	8	1	all xls 1.09
4b	HiAb(a)	715	8	1	xls, small amount glass 1.90
70	LoAb(a)	715	8	168	all xls 1.15
22	HiAb(a)	720	8	1.5	all glass
56	LoAb(a)	725	8+	72	xls + < 25% glass 1.06
5a	LoAb(a)	730	8	1	xls, v. small amount glass 1.11
5b	HiAb(a)	730	8	1	all glass
24	LoAb(a)	740	8	1.5	glass + < 1/2 xls
10	LoAb(a)	750	8	1	all glass
103	HiAb(a)	719	7.90	2.3	glass + < 1/2 xls
75a	LoAb(a)	728	6.05	431	all xls 1.14–1.17
49	HiAb(a)	730	6	1.5	v. rare glass
47	HiAb(a)	731	5.98	1.5	all xls
101	HiAb(a)	735	6.00	2	all xls
44	HiAb(a)	740	6	1.5	all glass

Table 1. (cont.)

73	LoAb(a)	740	6	168	xls + < 50% glass 1.10
50	HiAb(a)	741	6.10	1.5	all glass
81a	LoAb(a)	743	6.08	169	all xls 1.11
92a	LoAb(a)	749	6.00	166	xls + glass (~ 50-50) xls both lo and hi?
41	LoAb(a)	755	6	1.5	xls + rare glass
45	LoAb(a)	756	6.08	1.5	xls + some glass
39	LoAb(a)	765	6	1.5	glass + ~ 10% xls
40	LoAb(a)	765	6.10	1.5	glass + ~ 20% xls
99	HiAb(a)	738	4.97	2	all xls
100	HiAb(a)	743	5.10	2	all xls
96a	LoAb(a)	748	4.97	167	all xls
96b	LoAb(c)	748	4.97	167	all xls
96c	LoAb(b)	748	4.97	167	all xls
102	HiAb(a)	751	5.00	2	xls, trace glass
95a	LoAb(a)	754	5.00	167	xls, small amount glass xls both lo and hi
95b	LoAb(c)	754	5.00	167	xls + < 50% glass xls both lo and hi
7a	LoAb(a)	758	5.00	1	all xls 1.12
7b	HiAb(a)	758	5.00	1	all glass
17a	LoAb(a)	761	5.00	4.5	all xls 1.13
17b	MAb-15	761	5.00	4.5	glass + sparse xls
21a	LoAb(a)	761	5.03	8	all xls ~ 1.17
21b	MAb-15	761	5.03	8	xls + glass (~ 20%?)
18	LoAb(a)	760	5.00	136	glass + < 50% xls 1.13
61	LoAb(a)	748	4.30	209	all xls 1.13, some hi Ab?
87a	LoAb(a)	760	4.00	331	all xls lo and hi Ab (~ 1.15 + ~ 1.8)
82a	LoAb(a)	768	4.02	184	xls + ~ 10% glass lo and hi Ab
82b	HiAb(a)	768	4.02	184	xls + < 50% glass 1.84
74a	LoAb(a)	761	3.60	354	all xls lo and hi Ab (~ 1.10 + 1.85)
74b	HiAb(a)	761	3.60	354	all xls 1.85
63a	LoAb(a)	775	2.95	164	all xls lo Ab(1.10) + some hi Ab (1.82)
64b	HiAb(a)	775	2.95	164	all xls 1.85
60	HiAb(a)	779	2.95	1.5	all xls
69a	HiAb(a)	785	3.05	332	xls, Hi Ab, v. small amount glass
69b	MAb-20	785	3.05	332	xls, Hi Ab, v. small amount glass
69c	HiAb(a)	785	3.05	332	xls, Hi Ab, small amount glass
59	HiAb(a)	790	3.00	1.5	glass, some xls 1.86
66a	LoAb(a)	790	3.04	163	small amount glass Hi Ab(1.88) + Lo Ab(1.06)
66b	HiAb(a)	790	3.04	163	glass + some xls
52a	LoAb(a)	799	3.05	1.7	glass + sparse xls
52b	HiAb(a)	799	3.05	1.7	all xls 1.05
64	LoAb(a)	800	3.04	138	all glass
58	LoAb(a)	810	3.07	1.5	glass + xls (~ 50-50) 1.12, some Hi Ab?
54	LoAb(a)	800	2.50	130	all xls Hi Ab, 1.82
8a	LoAb(a)	841	2.00	1.8	xls + < 50% glass 1.07
8b	HiAb(a)	841	2.00	1.8	glass, some xls
53a	HiAb(a)	850	1.63	1.5	xls + ~ 20% glass
53b	MAb-20	850	1.63	1.5	xls + ~ 20% glass
53c	LoAb(a)	850	1.63	1.5	xls + < 20% glass Lo + some Hi Ab
51a	LoAb(a)	849	1.47	144	xls + small amount glass 1.91
51b	HiAb(a)	849	1.47	144	xls + small amount glass
19a	LoAb(a)	890	1.38	4	all glass
19b	MAb-15	890	1.38	4	all glass
12a	LoAb(a)	890	1.00	2	all xls Lo + some highish Ab
12b	HiAb(a)	890	1.00	2	xls + glass
13a	LoAb(a)	890	1.00	2	all xls Lo(1.05) + some high(1.83) Ab
13b	HiAb(a)	890	1.00	2	all xls 1.90
14	LoAb(a)	890	1.00	17.5	all xls ~ 1/2 Hi Ab, 1.82
27a	HiAb(a)	900	1.00	2	glass + some xls
27b	MAb-20	900	1.00	2	glass + some xls
27c	LoAb(a)	900	1.00	2	glass + some xls some Hi Ab
11a	LoAb(a)	937	1.00	2	all glass
11b	HiAb(a)	937	1.00	2	all glass
48	LoAb(a)	896	0.77	150	all xls euhedrons of Hi Ab 1.95
35a	LoAb(a)	948	0.70	1	glass + some xls
35b	MAb-20	948	0.70	1	glass + some xls
35c	HiAb(a)	948	0.70	1	glass + some xls
37a	LoAb(a)	949	0.55	1	xls + glass Lo + Hi Ab (2.0)
37b	MAb-20	949	0.55	1	xls + glass 2.02
37c	HiAb(a)	949	0.55	1	xls + glass 1.97
33	LoAb(a)	952	0.50	0.5	all xls some Hi Ab?
38a	LoAb(a)	1000	0.30	1	glass + some xls
38b	MAb-20	1000	0.30	1	glass + some xls
38c	HiAb(a)	1000	0.30	1	glass + some xls
46a	LoAb(a)	1000	0.26	1	xls, v. small amount glass Lo Ab + some Hi Ab(1.93)
46b	MAb-20	1000	0.26	1	xls, v. small amount glass 2.0
43	LoAb(a)	1000	0.25	1	xls, trace glass some hi Ab?

§ Listed in order of decreasing pressure.
* No. refers to Δ131 of xls in run product.
‖ Decimal values indicate gas vessel runs.
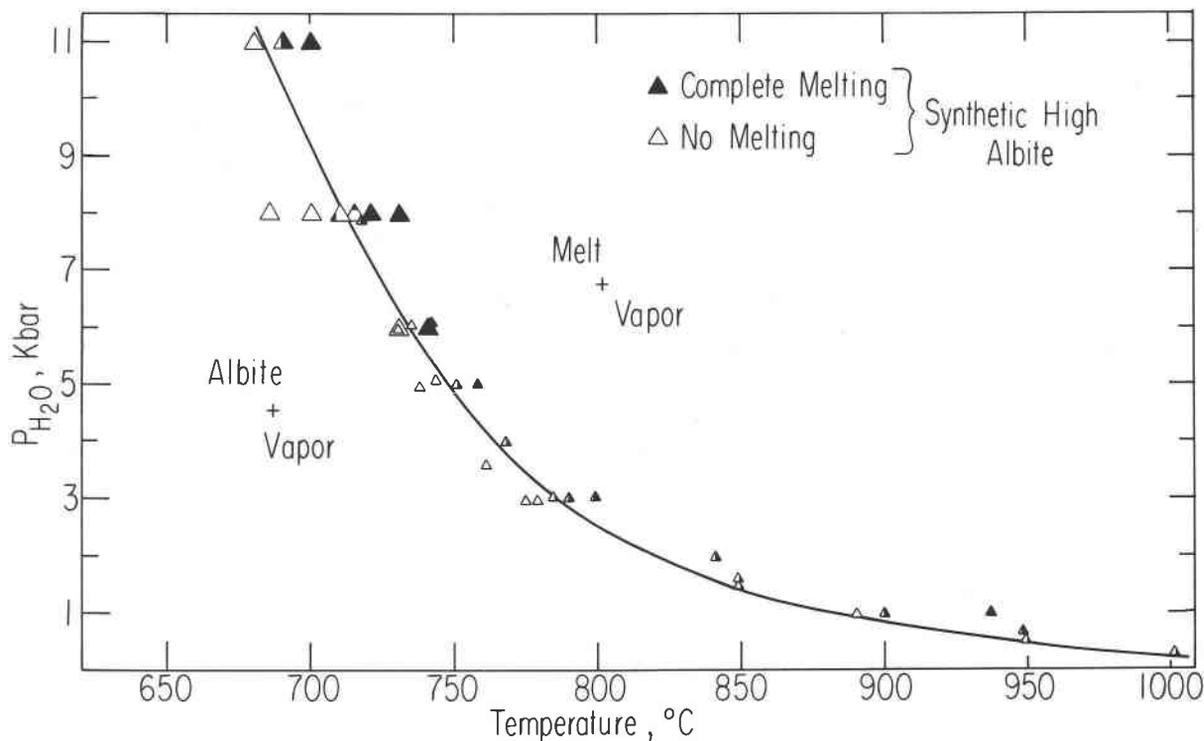
Fig. 2. The hydrothermal melting of synthetic high albite ($\Delta = 1.90$–1.92). Open triangles represent no melting, solid triangles complete melting, and partial melting is indicated by partially filled symbols. Larger triangles represent runs made in piston-cylinder devices, smaller triangles those done in internally heated gas vessels.

the value of $758°C \pm 3°C$ at 5.0 kbar obtained by Morse (1970) in cold-seal apparatus and calibrated internally heated gas-pressure apparatus ($754°C$ if a pressure correction of $+4°C$ to the thermocouple is removed) is dissonant with their data and with the values of Tuttle and Bowen extrapolated beyond 4 kbar. Our value at 5 kbar is very close to $750°C$.

The reasons for fairly large variation in the location of the solidus are not clear. Aside from errors in pressure and temperature measurement or control, or composition of the albite, differences might be related to detection of the first trace of melt, and perhaps, as will be seen in the following section, the structural state of the starting material.

Low albite

The data on the hydrothermal melting of low albite *as the starting material* are also presented in Table 1, and are plotted in Figure 3. We are not aware of any other determinations on hydrothermal melting of low albite. In Figure 4 the curves determined from both low and high albite are presented.

Several things are apparent from Figures 3 and 4 and from the data in Table 2:

1. The melting curve determined from low albite, unlike the high albite curve, has a pronounced inflection, which is

the result of an observed time-dependent melting behavior at temperatures above $745°C$.[2] Albite that is unmelted in short runs may melt to a significant extent in longer runs. For example, at $758°$ and 5 kbar, run 7a was all crystalline in one hour, and at $760°$ it was almost half melted in 136 hours. This behavior was not observed at 11 kbar ($\sim 700°$) and 8 kbar ($\sim 720°$), nor, as previously mentioned, was it observed in runs on high albite. The control in the gas vessels is good enough to obviate variations in temperature or pressure as contributing to the effect of time on degree of melting.

2. At temperatures below and pressures above the region of inflection, the low albite curve[3] lies at significantly

---

[2] The existence of an inflection is based on a pair of carefully controlled seven day gas-vessel experiments that bracket the curve at 6 kbar (MAb-91 and 92). A single run (MAb-73) done in piston-cylinder apparatus, is in conflict with this pair. The pressure and temperature measurement and control in the solid media device is not as good as in the internally heated gas vessel, especially in a seven day experiment at only 6 kbar. This point is therefore not plotted in Fig. 3.

[3] The phrase "low albite curve" will be used henceforth in place of the more accurate but awkward description "curve determined with low albite as the starting material."
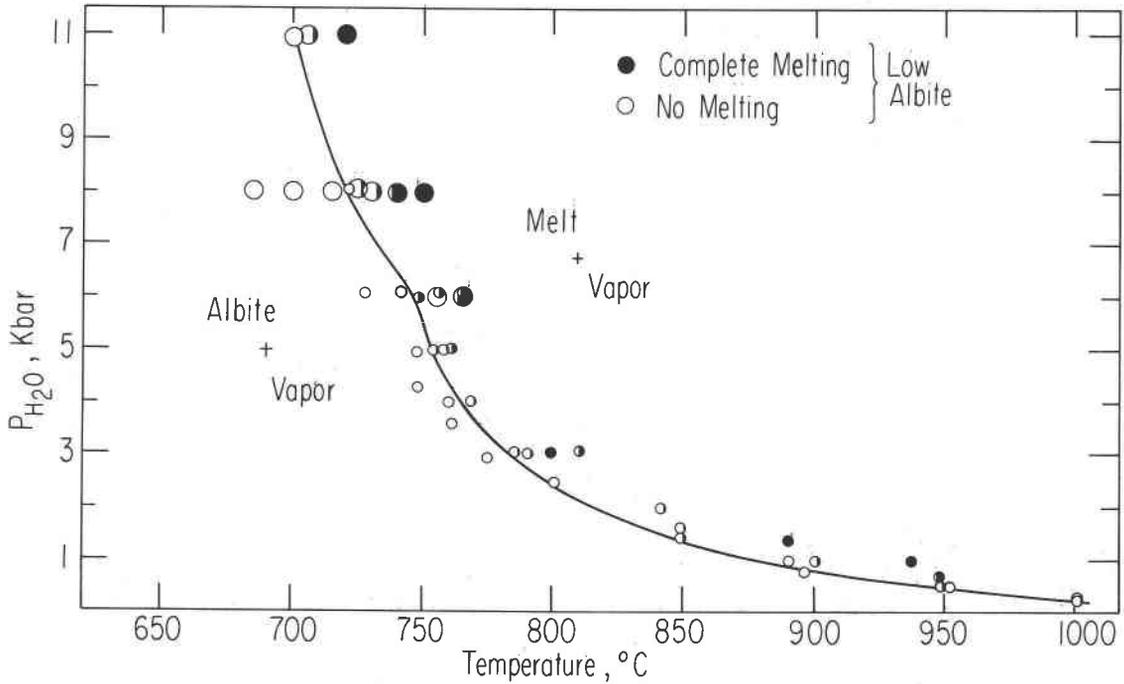
Fig. 3. The hydrothermal melting with low albite ($\Delta = 1.10$) used as starting material. Open circles represent no melting, solid circles complete melting, and partial melting is indicated by partially filled symbols. Large circles represent runs made in piston-cylinder devices, smaller circles those done in internally heated gas vessels. See text for discussion of time-dependence of melting behavior.
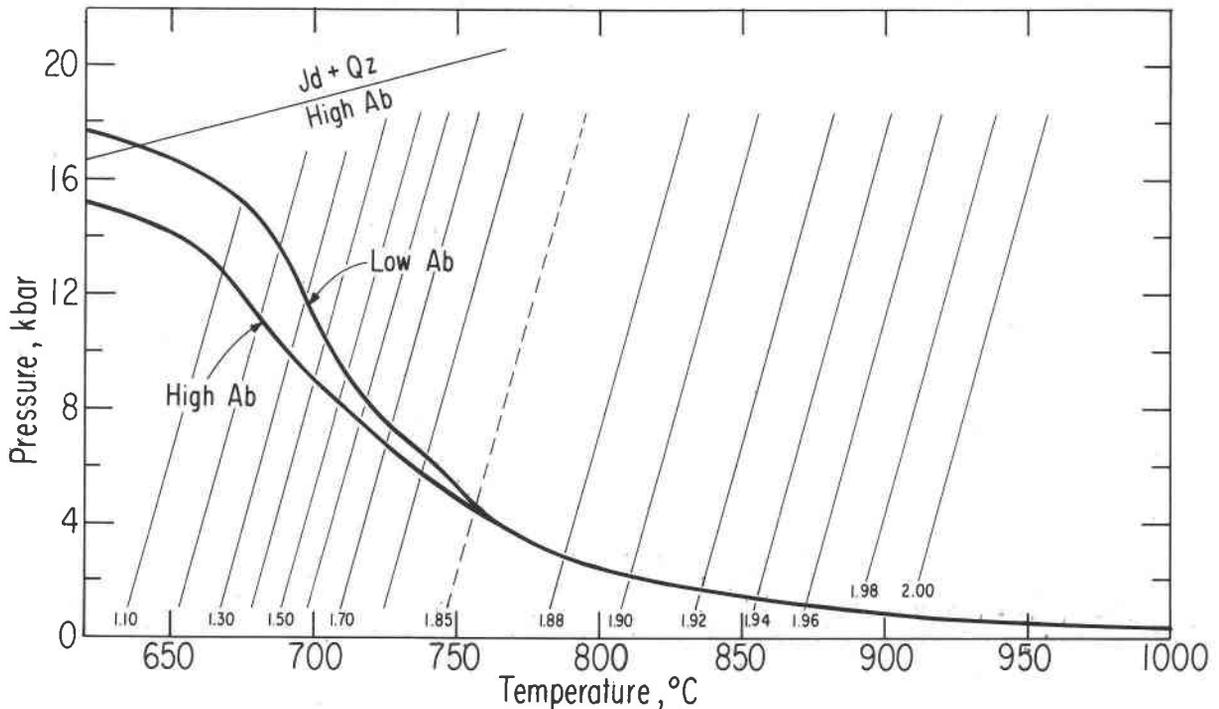
Fig. 4. Composite diagram of high albite melting curve (from Fig. 2) and curve determined from low albite starting material (from Fig. 3). High-pressure segments are from Fig. 5. Also shown is the high albite jadeite + quartz boundary after Holland (1980). Isopleths of structural state are plotted as straight lines, with slope of $dP/dT = 350$ bars/K, from Goldsmith and Jenkins (1985). Note change in isopleth spacings at $\Delta = 1.85$ (dashed line) and higher values.

higher temperatures than the high albite curve. The curves diverge with decreasing temperature and the difference at 14 kbar is approximately 30°C.

3. At temperatures above, and pressures below the region of inflection, the low albite curve becomes coincident with the high albite curve.

4. A "crossover", as in Figure 1, where the low albite curve would appear metastably at a lower temperature than the high albite curve is not observed. No melting of low albite has been detected in the *P–T* region below the high albite curve.

Melting pressures above 14 kbar

The higher pressure data on the hydrothermal melting of low and high albite are given in Table 1 and plotted in Figure 5. At pressures above approximately 14 kbar both solidus curves undergo a distinct flattening of the dP/dT slope. This greater pressure dependency produces melting at temperatures as low as 600°C as pressures approach the breakdown to jadeite plus quartz. In this region the solidus of low albite is close to 3 kbar above that of high albite.

In addition, the quenched melt-product has a texture quite unlike that of the lower pressure melts. It is not a coherent glass, but a soft powder, amorphous to X-rays.

Figure 6 is an SEM photograph of MAb-105, low albite run at 17 kbar, 680°C. The "powder" is made up of globules, mostly 2–5 microns in diameter. Small amounts of unmelted albite are present in this experiment, and one of the more obvious residual albite grains is apparent in Figure 6. Analysis of the globules and grains using a Kevex EDS system show them to have the albite stoichiometry. No attempt was made to determine the water content of this high-pressure melt product. Under the petrographic microscope it appears to be a somewhat brownish, isotropic "cloudy" material. It is less well defined than normal glass; the small particles are not clearly resolved. The melting interval may be larger at higher than at lower pressures.

Figure 5 also contains the curve for the reaction high albite = jadeite + quartz determined by Holland (1980). Newton and Smith (1967) and Hlabse and Kleppa (1968) considered the reaction low albite = jadeite + quartz, of interest in conjunction with Figure 5, but no reversed data are available. None of the runs plotted in Figure 5 were seeded with jadeite, and do not represent reversals. However, the three runs on low albite at pressures > 18 kbar show small amounts of jadeite, and a highly tentative breakdown curve for low albite is indicated. The observed
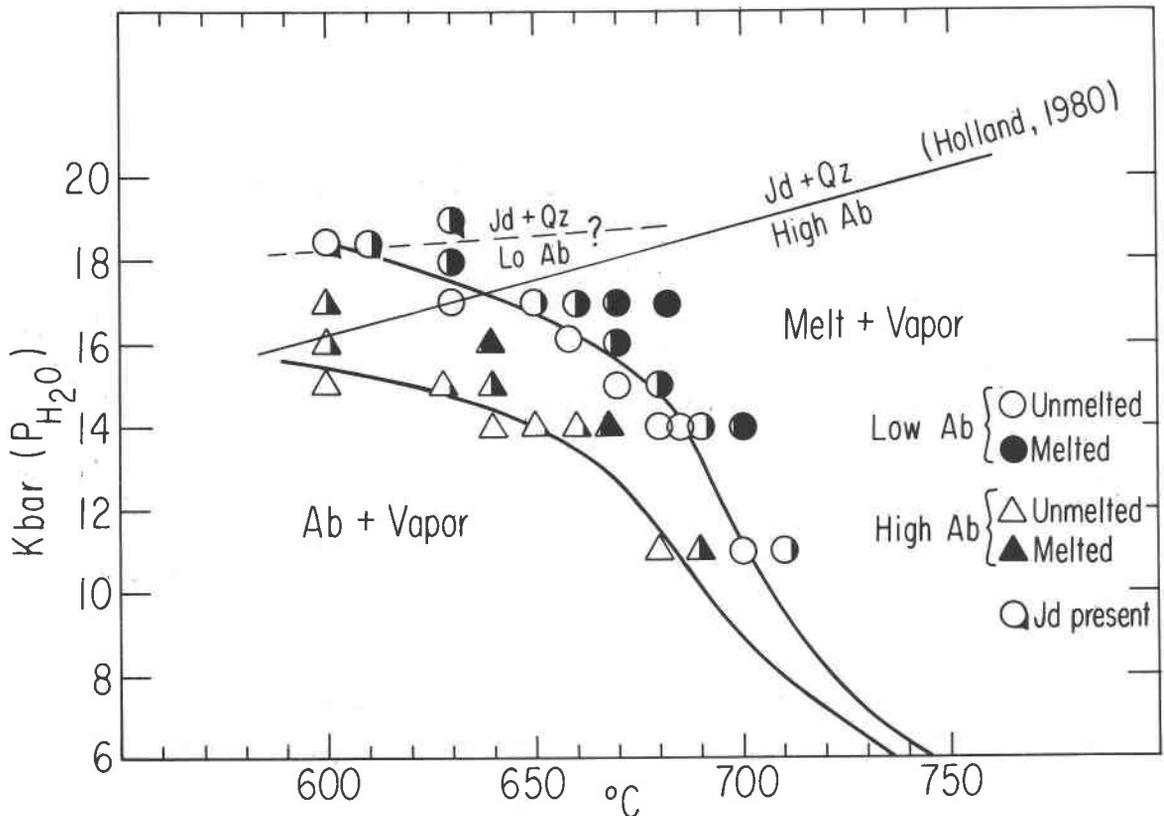
Fig. 5. The hydrothermal melting curves of high albite and low albite with data points at the higher pressures. The high albite jadeite + quartz boundary is after Holland (1980); the dashed line is a tentative boundary for the reaction low albite ⇌ jadeite + quartz (see text).
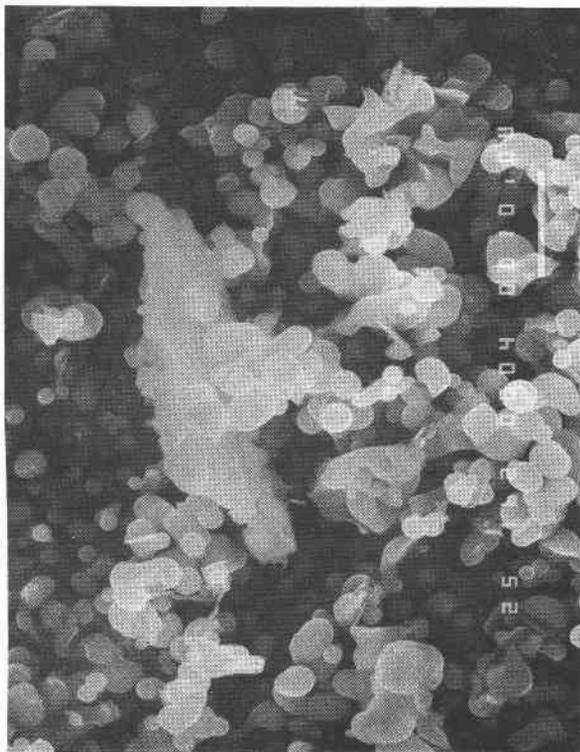
Fig. 6. SEM photograph of the product quenched from low albite starting material run at 17 kbar, 680° (MAb-105). The horizontal bar represents 10 μm. The large object is a residual crystal of albite.

change in properties of the hydrous liquids takes place at pressures not far below those at which 4-coordinated Al in albite changes to 6-coordination in jadeite.

Discussion

Implications of the melting curves

If a chemical and structural state equilibrium were established during hydrothermal treatment, the metastable limbs would not have been realized, and a single melting curve would have been produced. In a first-order transition, as illustrated in Figure 1, a single curve with a break in slope at the transition would have resulted. If the transition had taken place over a limited temperature interval, the break would have been smoothed into an inflection.

The establishment of structural state equilibrium by hydrothermal treatment in the pressure and temperature region of the transition has been shown in previous studies to be very difficult. The separation of the two curves in the lower temperature–higher pressure region (Figs. 4 and 5) clearly indicates that the degree of Al/Si order is essentially unchanged, even in the longer runs. It can, however, be concluded independently of the data of Goldsmith and Jenkins (1985) that at the higher temperatures where the

curves coalesce, high albite is stable. A number of the runs on low albite in this region show at least some high albite in the diffraction patterns, with or without glass being present (e.g. Nos. MAb-95a, 82a, 63a, 54).

The melting of high albite is presumed to be a relatively straightforward conversion of an Al/Si disordered crystalline network to a more random disordered (even if) highly polmerized melt. Water helps depolymerize the liquid, but on a short-term basis has rather little effect on the structural state of the solid. But in what way does *low* albite melt? Does it disorder completely to high albite, and melt as the disordered modification, or can it be induced to go directly or abruptly to the disordered liquid? It is possible that runs which produced low albite coexisting with a glass at temperatures above the region of inflection (i.e., MAb-18) are examples of the partial conversion of low albite to high albite with subsequent melting of the high albite. Unfortunately we do not see how to reconstruct the history of the crystals that have melted. It is, however, reasonable that low albite which does not melt in a matter of hours, but that does melt in significantly longer times under the same $P(H_2O)–T$ conditions, is slowly disordering, and is therefore at a temperature above the equilibrium structural state of the starting material.

The absence of a detectable metastable extension of the low albite melting curve beneath the high albite curve may be a consequence of the low albite melting process. If disordering is a precursor to melting, the metastable extension would not be realized. The evidence points to this conclusion. We are not, however, prepared to consider the broader aspects of melting, which involves comparing the behavior of compounds that may retain most of their Al/Si order up to the melting point, such as anorthite (Goldsmith and Laves, 1955; Laves and Goldsmith, 1955), to the "polymorphic" behavior of albite.

Structural state and melting equilibria

Figure 4 illustrates the fact that hydrothermal melting behavior is related to the structural state of the albite and that each structural state, in the absence of change during the run, will have its own hydrothermal melting curve. It is also likely that dry melting at one atmosphere, if rapid enough to avoid further disordering, would show melting temperatures that varied with structural state of the starting material. The investigation involving direct reversal of degree of order (Goldsmith and Jenkins, 1985) can be used, to better understand the extent to which structural state equilibrium or disequilibrium may effect the curves.

Figure 4 contains, in addition to the hydrothermal melting curves, isopleths of structural state obtained from the data in Figure 1 of Goldsmith and Jenkins (1985) using a value of $dP/dT = 350$ bars/K. The $\Delta = 1.85$ isopleth, the value at which the rate of change of the disorder in albite has slowed and which is at 790–800°C at 17–18 kbar, cuts the melting curves near 760° and 4.5 kbar, essentially at the coalescence of the curves determined from high albite and low albite. The degree of order represented by $\Delta 131 = 1.85$

is also that value at which the rate of change of order with temperature undergoes a large decrease (Goldsmith and Jenkins, 1985, Fig. 1). The coincidence of these two observations justify a definition of high albite as albite with $\Delta 131 = 1.85$. At temperatures greater than 760°C, the single curve probably represents the equilibrium hydrothermal melting curve for those high albites that are stable at temperatures > 760°. The data in Table 1 tend to substantiate the view that at temperatures > 760° the hydrothermal conversion of low albite to high albite is rapid enough that the melting of a high albite determined the liquidus, even if residual low albite remains. The $\Delta 131$-value of the highly disordered albites in equilibrium with the melting curve should increase with $T° > 760°$ to values > 1.85 as indicated by the isopleths in Figure 4.

The lower-temperature limb of Figure 4, the high albite curve, is certainly not in equilibrium with melt, and is a relic of the slowness of the ordering process even under the lower temperature but higher $P(H_2O)$ conditions. The time-dependency of melting of low albite has been pointed out, particularly in the temperature range 740–760°C. Little change of behavior with time is observed at lower temperatures. If equilibrium were presumed, the interpretation could be that the curve at temperatures below approximately 740° represented stable low albite, and that in the 740–760°C region intermediate albites were stable. The isopleths of $\Delta 131$ show, however, that at all temperatures down to approximately 680°C, intermediate albites are stable, and that at the pressures of the melting curves, the range of intermediate albites extends from ~680° to ~760°C. Certainly at temperatures <650°C low albite is stable, as is this portion of the low albite curve. The significantly more refractory nature of low albite compared to high albite at these low temperatures may be a consequence of the fact that at low temperatures low albite must melt as an ordered compound. The separation of the curves is an expression of the energetic difference of the two states of Al/Si order.

It may be that the T region of time-dependent melting exists only because the rate of Al/Si hydrothermally induced change in structural state is rapid enough to be observed in the time allotted to the experimental runs, and at temperatures below ~740°C it is too slow for even the very patient investigator. The region of inflection is thus almost certainly an expression of kinetic, not equilibrium behavior, for the equilibrium transition takes place over the entire lower temperature region of the determined curves. The equilibrium melting curve, at temperatures below 760°C, lies somewhere between the two curves of Figure 4.

It was noted that in the region of 5–10 kbar, the curve of Bohlen et al. (1982) is at lower temperatures than our high albite curve. Bohlen et al. heated their synthetic albite at 1100°C for 24 hours before determining the melting curve. No $\Delta 131$-value or measure of disorder of the albite was given, but it is possible that their melting curve was determined with material of a higher structural state than that in Figure 2. It is not likely, however, that the difference between the curve of Bohlen et al. (1982) and that of Figure 2 could be due entirely to this effect, based on the spread between high and low albite in Figure 4.

Albite liquid above 14 kbar

The observed melting behavior of albite at pressures greater than 14 kbar calls for comment, even if premature. It is well known that water depolymerizes silicate melts (c.f. Burnham, 1975), and that water content of melts increases with $P(H_2O)$. Large decreases in viscosity in highly polymerized melts such as albite are the result of the disruption of the melt framework by interaction of H_2O with bridging oxygens to form OH groups and a less polymerized melt. Stolper (1982) presents evidence for the existence of molecular water in solution as well as hydroxyl groups, and also for an increase in the proportion of molecular water with increase in H_2O concentration in the melt. At pressures > 10 kbar (> 15 wt.% water) Stolper (1982) states that most of the dissolved water is present as molecular water. Thus the initial extensive depolymerization produced by the hydroxyl groups at low water concentration becomes decreasingly effective as concentration increases, and melt viscosity, which dramatically decreases as water is first added, should show less of a decrease with additional increments of water. This prediction does not explain our observations in this study at $P(H_2O) > 14$ kbar.

The H_2O content of the high pressure liquids in this study has not been determined. Burnham and Davis (1974) show a value of 16.5 wt.% water in the saturated albite melt at 700°C and 10 kbar; at higher pressures and lower temperatures the value must be significantly greater. The value of 16.5 wt.% translates to 74 mol percent; it would appear that at the higher pressures the "melt" is a low-density rather tenuous fluid. The flattening of the solidii may even indicate an approach to maxima on the three-phase curves, as observed in $K_2Si_2O_5$ (Morey and Fenner, 1917).

Cation coordination must also be considered, particularly as effected by the presence of water. A coordination change of Al from 4 to 6 in *anhydrous* aluminosilicate liquids, which would induce depolymerization, has been proposed to explain the observed decrease in viscosity of aluminosilicate melts at high pressures (Kushiro, 1976; 1978). No evidence for octahedral Al has been found in a number of investigations of Al-containing glasses quenched at high pressures (Sharma et al., 1979; Sharma and Simons, 1981) or even in the more favorable case of gallium-containing glasses (Fleet et al., 1984). There is no assurance, however, that a coordination change would be preserved during the quench, and in situ observations at high pressures and temperatures have not been carried out.

The presence of hydroxyl groups in place of oxygen atoms around Al and Si should favor higher coordination. Hydroxyl units are associated with Al, not Si, in aluminosilicates, normally with the Al in 6 coordination. The OH group has a smaller charge than oxygen, and higher coordination is aided by reducing repulsion among the coordinating atoms (Goldsmith, 1953).

References

Boettcher, A. L. and Wyllie, P.J. (1969) Phase relationships in the system $NaAlSi_3O_8-SiO_2-H_2O$ to 35 kilobars pressure. American Journal of Science, 267, 875–909.

Bohlen, S. R., Boettcher, A. L. and Wall, V. J. (1982) The system albite–H_2O–CO_2; a model for melting and activities of water at high pressures. American Mineralogist, 67, 451–462.

Burnham, C. W. (1975) Water and magmas: a mixing model. Geochimica et Cosmochimica Acta, 19, 1077–1084.

Burnham, C. W. and Jahns, R. H. (1962) A method for determining the solubility of water in silicate melts. American Journal of Science, 260, 721–745.

Fleet, M. E., Herzberg, C. T., Henderson, G. S., Crozier, E. D., Osborne, M. D. and Scarfe, C. M. (1984) Coordination of Fe, Ga and Ge in high pressure glasses by Mossbauer, Raman and X-ray absorption spectroscopy, and geological inplications. Geochimica et Cosmochimica Acta, 48, 1455–1466.

Goldsmith, J. R. (1953) A "simplexity principle" and its relation to "ease" of crystallization. Journal of Geology, 61, 439–451.

Goldsmith, J. R. and Jenkins, D. M. (1985) The high-low albite relations revealed by reversal of degree of order at high pressures. American Mineralogist, 70, 911–923.

Goldsmith, J. R. and Laves, F. (1955) Cation order in anorthite ($CaAl_2Si_2O_8$) as revealed by gallium and germanium substitutions. Zeitschrift für Kristallographie, 106, 213–226.

Goranson, R. W. (1938) Silicate–water systems: Phase equilibria in the $NaAlSi_3O_8-H_2O$ and $KAlSi_3O_8-H_2O$ systems at high temperatures and pressures. American Journal of Science, 35-A, 71–91.

Hlabse, T. and Kleppa, O. J. (1968) The thermochemistry of jadeite. American Mineralogist, 53, 1281–1292.

Kushiro, I. (1976) Changes in viscosity and structural changes of albite ($NaAlSi_3O_8$) melt at high pressures. Earth and Planetary Science Letters, 41, 87–90.

Laves, F. and Goldsmith, J. R. (1955) The effect of temperature and composition on the Al–Si distribution in anorthite. Zeitschrift für Kristallographie, 106, 227–235.

Luth, W. C., Jahns, R. H. and Tuttle, O. F. (1964) The granite system at pressures of 4 to 10 kilobars. Journal of Geophysical Research, 69, 759–773.

Morey, G. W. (1957) The solubility of solids in gases. Economic Geology, 52, 225–251.

Morey, G. W. and Fenner, C. N. (1917) The ternary system $H_2O-K_2SiO_3-SiO_2$. Journal of the American Chemical Society, 39, 1173–1229.

Morse, S. A. (1970) Alkali feldspars with water at 5 kb pressure. Journal of Petrology, 11, 221–251.

Newton, R. C. and Smith, J. V. (1967) Investigations concerning the breakdown of albite at depth in the earth. Journal of Geology, 75, 268–286.

Sharma, S. K. and Simons, B. (1981) Raman study of crystalline polymorphs and glasses of spodumene composition quenched from various pressures. American Mineralogist, 66, 118–126.

Sharma, S. K., Virgo, D. and Mysen, B. O. (1979) Raman study of the coordination of aluminum in jadeite melts as a function of pressure. American Mineralogist, 64, 779–787.

Sosman, R. B. (1927) The properties of silica. American Chemical Society Monograph Series, p. 89–92. The Chemical Catalogue Company, New York.

Stolper, E. (1982) The speciation of water in silicate melts. Geochimica et Cosmochimica Acta, 46, 2609–2620.

Tuttle, O. F. and Bowen, N. L. (1958) Origin of granite in the light of experimental studies in the system $NaAlSi_3O_8-KAlSi_3O_8-SiO_2-H_2O$. Geological Society of America, Memoir 74.

Yoder, H. S., Jr. (1958) Effect of water on the melting of silicates. Carnegie Institution of Washington Year Book, 57, 189–191.